Oncologie

Tech Science Press

DOI: 10.32604/Oncologie.2021.015520

ARTICLE

Application Value of Multi-Slice Spiral CT Multiplanar Reconstruction Technique in the Diagnosis and Clinicopathological Analysis of Gastrointestinal Lymphoma

Yongtao Yu and Guangdong Zou*

Department of Radiology, Linyi Central Hospital, Linyi, 276402, China

*Corresponding Author: Guangdong Zou. Email: linyizouguangdong@163.com

Received: 24 December 2020 Accepted: 10 March 2021

ABSTRACT

Objective: The purpose was to explore the value of multi-slice spiral CT (MSCT) multiplanar reconstruction technique in the diagnosis and clinicopathological analysis of gastrointestinal lymphoma (GIL). **Methods:** 82 GIL patients treated in our hospital from February 2018 to February 2019 were selected as the experimental group of this study, and 82 patients with other gastrointestinal tumors diagnosed by pathology during the same period were selected as the control group. Both groups of patients were scanned by MSCT and analyzed by multiplanar reconstruction technique to compare the diagnostic results and clinicopathological indexes of the two groups. **Results:** The diagnostic accuracy of MSCT multiplanar reconstruction scanning was higher, with no statistical difference from that of pathological examination results ($P > 0.05$). Compared with the control group, the objective image noise of the experimental group was lower while the signal-to-noise ratio (SNR) was higher, with significant differences between the two groups ($P < 0.05$). There were statistically significant differences in the CT reconstruction parameters of different tumor types and different clinical stages in the experimental group ($P < 0.05$). **Conclusion:** MSCT multiplanar reconstruction technique is effective in diagnosing GIL, and the CT reconstruction parameters have important guiding value for the differentiation of tumor tissue types and clinical stages. The technique enables the doctors to fully grasp the clinical manifestations of the disease and select appropriate therapeutic regimens, improving the diagnostic accuracy and prognostic effect of the disease, which is worthy of wide application and promotion in clinic.

KEYWORDS

Multi-slice spiral CT; multiplanar reconstruction technique; gastrointestinal lymphoma; pathological analysis

1 Introduction

Gastrointestinal lymphoma (GIL) is a lymphoma that occurs in the gastrointestinal tract such as stomach, esophagus, small intestine and large intestine, among which gastric lymphoma has the highest incidence [1–3]. The disease begins with the transformation of immunocompetent cells at different stages or the disturbance of the regulatory mechanism *in vivo*, which leads to the abnormal differentiation or proliferation of lymphocytes, resulting in tissue lesions. GIL is divided into primary GIL and secondary GIL in clinical treatment, and the former is more common. Due to the occult onset of GIL, the clinical symptoms of patients are easily confused with other tumors, which leads to misdiagnosis or deterioration of disease and poor prognosis. Therefore, correct diagnosis is the key to improve the prognosis of patients in the clinical treatment of this disease. Since earlier clinical stages show better prognosis in treatment, early diagnosis is particularly important. In recent years, with the deepening of medical research, medical imaging technique is developing rapidly and has become a common examination method in clinical treatment [4,5]. While computed tomography (CT) is often used in the examination of gastrointestinal diseases, conventional CT examination is difficult to identify the complex structure of the gastrointestinal tract, leading to poor clinical diagnosis. Multi-slice spiral CT (MSCT) multiplanar reconstruction technique has certain improvement compared with conventional scanning, but there is a lack of in-depth study on its effect on the diagnosis of GIL. Therefore, this experiment mainly explored the application value of MSCT multiplanar reconstruction technique in the diagnosis and clinicopathological analysis of GIL, summarized and reported as follows.

2 Materials and Methods

2.1 General Information

82 GIL patients treated in our hospital from February 2018 to February 2019 were selected as the experimental group of this study, and 82 patients with other gastrointestinal tumors diagnosed by pathology during the same period were selected as the control group. The experimental group included 42 cases of diffuse large B-cell lymphoma, 23 cases of mucosa-associated lymphoma, 10 cases of small B-cell lymphoma and 7 cases of mantle cell lymphoma. There was no significant difference in general data between the two groups of patients ($P > 0.05$), as shown in Tab. 1.

Table 1: Comparison of the general information between two groups of patients (n = 82 in each group)

		Experimental group	Control group	t or X^2	*P*
Age (years old)		54.16 ± 6.85	53.08 ± 7.62	0.9545	0.3413
Course of disease (years)		2.41 ± 0.26	2.37 ± 0.32	0.8785	0.3810
Clinical staging	Stages I–II	24(29.27)	21(25.61)	0.2756	0.600
	Stages II–IV	58(70.73)	61(74.39)		
Medical history	Hypertension	23(20.05)	15(18.29)	0.3902	0.532
	Diabetes mellitus	20(24.39)	24(29.27)		
	No	39(47.56)	43(52.44)		
Smoking	Yes	27(32.93)	25(30.49)	0.1126	0.737
	No	55(67.07)	57(69.51)		
Drinking	Yes	44(53.66)	47(57.32)	0.2222	0.637
	No	38(46.34)	35(42.68)		
Gender	Male	48(58.54)	43(52.44)	0.6172	0.432
	Female	34(41.46)	39(47.56)		
Residence	Urban areas	51(62.19)	56(68.29)	0.6722	0.412
	Rural areas	31(37.81)	26(31.71)		

2.2 Inclusion Criteria

(1) GIL or other gastrointestinal tumors confirmed by pathological study; (2) Complete clinical records of patients; (3) This study was approved by the hospital ethics committee, and the patients and their families knew the purpose and process of this experimental study, and signed the informed consent.

2.3 Exclusion Criteria

(1) Patients with brain, heart, kidney, liver and other organ and tissue lesions; (2) Patients with secondary GIL; (3) Patients who were allergic or contraindicated to iohexol injection used for MSCT multiplanar reconstruction; (4) Patients who had mental and other cognitive impairment or refused to cooperate with the experiment.

2.4 Methods

All patients needed to fast for 8 hours before MSCT multiplanar reconstruction, and took oral administration of 100–600 ml of meglumine diatrizoate (2%–3%) before scanning to fully expand the gastrointestinal tract. The patients took a supine position and breathed evenly [6]. Brilliance spiral CT (64 rows; manufacturer: Philips) was used to scan the patients from the diaphragmatic surface of liver to the upper edge of pubic symphysis, with the scanning parameters including 3.1 of pitch, 5 mm of slice thickness, 5 mm of reconstruction interval, 512 × 512 of matrix, 64 × 0.625 mm of collimator window width and 2 mm^2 of region of interest (ROI) area [7,8]. After the scanning was completed, non-ionic contrast agent iohexol injection (manufacturer: General Electric Pharmaceutical (Shanghai) Co., Ltd., Shanghai, China; SFDA approval No. H20084191) was injected into the antecubital vein at a dose of 1.5 mL/kg and a speed of 3.5 mL/s. The delayed contrast enhanced CT scan was performed at 26–180 s after the injection of the contrast [9–12]. The data of ROI were transmitted to the workstation for analysis and processing. After observing the lesion thickness, plain CT value, enhanced CT value, peripheral lymph nodes and retroperitoneal lymph nodes, four radiologists with more than five years of clinical experience performed the multiplanar reconstruction and issued the analysis report.

2.5 Observation Indexes

Subjective evaluation of image quality was shown in the following table. Analysis was conducted on the relevant imaging data of the same patient to evaluate the quality of reconstruction images by professional doctors on a 5-point scale.

Score	Evaluation criteria
1	Images with poor quality which could not be used for diagnosis
2	Images with poor quality, large noise and many artifacts
3	Images which were acceptable in image definition and could be used for diagnosis, with general quality
4	Images with clear image display and good quality
5	Images which had good anatomical details and fully met the needs of diagnosis, with excellent quality

Objective evaluation of image quality. The ROI was selected to calculate the standard deviation (SD) of objective image noise and (SNR).

2.6 Statistical Processing

The data obtained in this study were statistically analyzed and processed by SPSS20.0 software. The count data were tested by X^2, expressed by [n(%)], and the measurement data were measured by *t* test, expressed by ($\bar{x} \pm s$). The difference was statistically significant when $P < 0.05$.

3 Results

3.1 Diagnostic Accuracy of MSCT Multiplanar Reconstruction Scanning

The diagnostic accuracy of MSCT multiplanar reconstruction scanning was higher, with no statistical difference from that of the pathological examination results ($P > 0.05$), as detailed in Tab. 2.

Table 2: Comparison of diagnostic accuracy of MSCT multiplanar reconstruction and pathological examination (n = 82, %)

Category	Large B-cell lymphoma	Mucosa-associated lymphoma	Small B-cell lymphoma	Mantle cell lymphoma
Pathological examination	42	23	10	7
MSCT multiplanar reconstruction	42(100)	22(95.65)	10(100)	7(100)
X^2	0.000	1.022	0.000	0.000
P	1.000	0.312	1.000	1.000

3.2 Comparison of CT Reconstruction Parameters between Two Groups of Patients

The CT reconstruction parameters of the experimental group were significantly better than those of the control group, with statistical significance, as shown in Fig. 1.

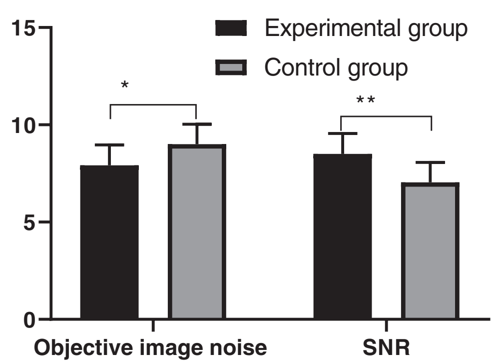

Figure 1: Comparison of CT reconstruction parameters between two groups of patients ($\bar{x} \pm s$). Note: The abscissa represents CT reconstruction parameters (objective image noise and SNR), and the ordinate represents parameter values. The objective image noise and SNR were (7.92 ± 1.05) and (8.51 ± 1.04) respectively in the experimental group. The objective image noise and SNR were (9.01 ± 1.02) and (7.04 ± 1.03) respectively in the control group. *indicated that there was a significant difference in the objective image noise between the two groups of patients ($t = 6.7427$, $P = 0.000$). ** indicated that there was a significant difference in the SNR between the two groups of patients ($t = 9.0942$, $P = 0.000$)

3.3 Comparison of CT Reconstruction Parameters of Different Tumor Types in the Experimental Group

The objective image noise of four different gastrointestinal lymphomas in the experimental group was detailed in Fig. 2, and the SNR was detailed in Fig. 3. There were statistically significant differences in objective noise and SNR of the four different gastrointestinal lymphomas in the group.

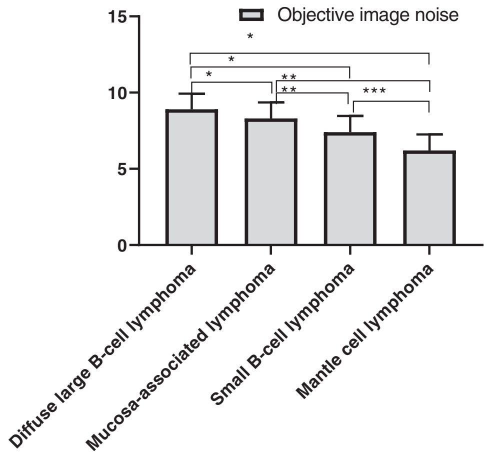

Figure 2: Comparison of objective image noise of the four different gastrointestinal lymphomas (x̄ ± s). Note: The abscissa represents the types of gastrointestinal lymphoma (diffuse large B-cell lymphoma, mucosa-associated lymphoma, small B-cell lymphoma and mantle cell lymphoma, respectively), and the ordinate represents the objective image noise. The objective image noise of the diffuse large B-cell lymphoma, mucosa-associated lymphoma, small B-cell lymphoma and mantle cell lymphoma was (8.9 ± 1.02), (8.31 ± 1.05), (7.40 ± 1.07) and (6.20 ± 1.05), respectively. * from bottom to top indicated that the objective image noise of diffuse large B-cell lymphoma was significantly different from that of mucosa-associated lymphoma, small B-cell lymphoma and mantle cell lymphoma (t = 2.2444, 4.1697 and 6.4833; P = 0.0283, 0.0001 and 0.000). ** from bottom to top indicated that the objective image noise of mucosa-associated lymphoma was significantly different from that of small B-cell lymphoma and mantle cell lymphoma (t = 2.2753 and 6.553; P = 0.03 and 0.0001). *** indicated a significant difference in the objective image noise between small B-cell lymphoma and mantle cell lymphoma (t = 2.2928, P = 0.0367)

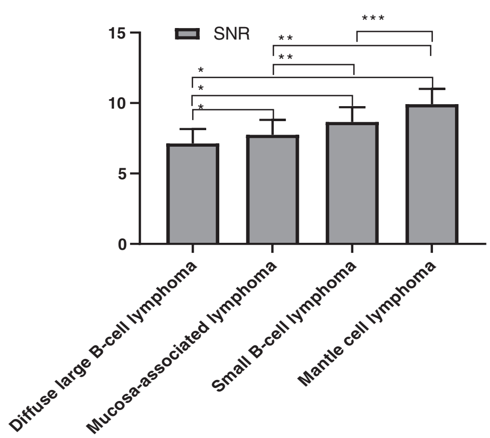

Figure 3: Comparison of the SNR of four gastrointestinal lymphomas (x̄ ± s). Note: The abscissa represents the types of gastrointestinal lymphoma (diffuse large B-cell lymphoma, mucosa-associated lymphoma, small B-cell lymphoma and mantle cell lymphoma respectively), and the ordinate represents the SNR. The SNR of the diffuse large B-cell lymphoma, mucosa-associated lymphoma, small B-cell lymphoma and mantle cell lymphoma was (7.13 ± 1.02), (7.74 ± 1.07), (8.66 ± 1.05) and (9.92 ± 1.08), respectively. * from bottom to top indicated that the SNR of diffuse large B-cell lymphoma was significantly different from that of mucosa-associated lymphoma, small B-cell lymphoma and mantle cell lymphoma (t = 2.6661, 4.2403 and 6.64893; P = 0.0269, 0.0001 and 0.000). ** from bottom to top indicated that the SNR of mucosa-associated lymphoma was significantly different from that of small B-cell lymphoma and mantle cell lymphoma (t = 2.2822 and 4.7103; P = 0.0295 and 0.0001). *** indicated a significant difference in the SNR between small B-cell lymphoma and mantle cell lymphoma (t = 2.4073, P = 0.0294)

3.4 Comparison of CT Reconstruction Parameters of Patients with Different Clinical Stages in the Experimental Group

The comparison of CT reconstruction parameter (objective image noise) of different clinical stages in the experimental group was detailed in Fig. 4, and the SNR comparison was detailed in Fig. 5. There were statistically significant differences in the objective noise and SNR of the four different clinical stages in the experimental group.

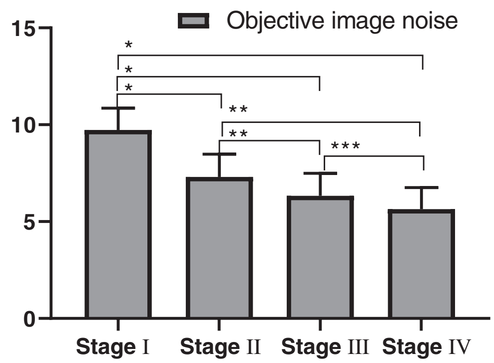

Figure 4: Comparison of objective image noise in patients with different clinical stages (x̄ ± s). Note: The ordinates represent different clinical stages of patients in the experimental group (Stages I–IV), and the ordinate represents the objective image noise. The objective image noise was (9.73 ± 1.12), (7.31 ± 1.17), (6.33 ± 1.16) and (5.64 ± 1.12) respectively in patients with Stages I, II, III and IV. * from bottom to top indicated that the objective image noise of Stage I was significantly different from that of Stage II, Stage III and Stage IV (t = 4.9819, 7.9149 and 9.2291; P = 0.001, 0.000 and 0.000). ** from bottom to top indicated that the objective image noise of Stage II was significantly different from that of Stage III and Stage IV (t = 2.7423 and 4.3739; P = 0.0085 and 0.0001). *** indicated a significant difference in the objective image noise of patients between Stage III and Stage IV (t = 2.2265, P = 0.03)

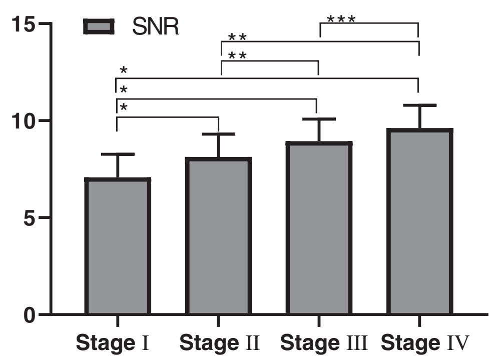

Figure 5: Comparison of SNR of patients with different clinical stages (x̄ ± s). Note: The ordinates represent different clinical stages of patients in the experimental group (Stages I–IV), and the ordinate represents the SNR. The SNR was (7.08 ± 1.19), (8.13 ± 1.18), (8.95 ± 1.13) and (9.62 ± 1.17) respectively in patients with Stages I, II, III and IV. * from bottom to top indicated that the SNR of Stage I was significantly different from that of Stage II, Stage III and Stage IV (t = 2.1039, 4.3961 and 5.4606; P = 0.047, 0.0001 and 0.000). ** from bottom to top indicated that the SNR of Stage II was significantly different from that of Stage III and Stage IV (t = 2.3029 and 3.7903; P = 0.0256 and 0.0006). *** indicated a significant difference in the SNR of patients between Stage III and Stage IV (t = 2.1389, P = 0.0368)

4 Discussion

GIL is not a common gastrointestinal tumor disease, so its treatment is different from that of other gastrointestinal tumors [13–16]. With the deepening of clinical research, the causes of GIL have become increasingly clear, including human immunodeficiency virus infection, immunosuppression, celiac disease, etc. As the clinical stage of the disease develops, patients will be accompanied by nausea, vomiting, hematemesis, abdominal pain and other uncomfortable conditions that are similar with those of other gastrointestinal diseases, easily causing misdiagnosis [17–20]. GIL originates from lymphoid tissue of the mucosa lamina propria or submucosa. But routine examination is difficult to find the lesions, and most patients are diagnosed after surgical resection. Therefore, a reliable examination method is needed to assist doctors in diagnosing the disease in the clinical treatment.

Medical imaging is a common examination method in clinical diagnosis, and CT, X-ray and ultrasound are typical methods for diagnosis of GIL. Conventional CT examination can display the general morphology of the gastrointestinal tract well, but is unsatisfactory in showing the gastrointestinal wall, mucosal folds and gastrointestinal cavity if atrophy occurs the gastrointestinal tract, which is difficult to meet the diagnostic needs. In addition, the gastrointestinal tract has certain complexity and gas, so the methods above are not ideal in the diagnosis of GIL. With high definition and resolution, MSCT technique will significantly improve the image quality with the combination of multiplanar reconstruction technique [21,22]. Based on this, this experiment not only selected MSCT multiplanar reconstruction technique to better determine the location, size of tumor lesions and the relationship with other tissues, but also used relevant algorithms to process noise and improve image quality. The study showed that the diagnostic accuracy of MSCT multiplanar reconstruction scanning was higher, indicating that MSCT multiplanar reconstruction has a better diagnostic effect on GIL. Compared with the control group, the objective image noise of the experimental group was lower while the SNR was higher, with significant differences between the two groups. In the diagnosis of other gastrointestinal tumors such as leiomyoma by MSCT multiplanar reconstruction technique, the objective image noise was significantly lower than that of GIL. Therefore, MSCT multiplanar reconstruction technique enables the diagnosis of GIL to be significantly different from that of other gastrointestinal tumors. There were statistically significant differences in the CT reconstruction parameters of different tumor types and different clinical stages in the experimental group, indicating that the analysis of MSCT multiplanar reconstruction parameters was helpful for detecting the tissue types and clinical stages of GIL, especially accurately determining the clinical stages, which was of great significance for the selection of therapeutic regimens and prognosis. The results of this study are consistent with those of Takata et al. [23] who stated that MSCT multiplanar reconstruction technique for GIL examination could not only accurately find the lesions, but also obtain more tumor information, which improved the image definition, and provided reference and convenience for clinical diagnosis of GIL.

In conclusion, MSCT multiplanar reconstruction technique is effective in diagnosing GIL, and the CT reconstruction parameters have important guiding value for the differentiation of tumor tissue types and clinical stages. The technique improves the diagnostic accuracy, and enables the doctors to fully master the clinical manifestations of the disease and select appropriate therapeutic regimens, which is worthy of wide application and promotion in clinic. Since this is a monocentric study with a small sample size, the diagnostic value of MSCT multiplanar reconstruction technique for GIL needs further confirmation from multi-center studies with a larger sample size and randomized controlled trials.

Funding Statement: The authors received no specific funding for this study.

Conflicts of Interest: The authors declare that they have no conflicts of interest to report regarding the present study.

References

1. Sang, L., Zhou, Z., Wu, C. (2019). Diagnosis of pulmonary embolism by treatment based on analysis of multi-slice spiral CT pulmonary artery images. *Journal of Medical Imaging and Health Informatics, 9(5),* 867–872. DOI 10.1166/jmihi.2019.2683.
2. Wang, M., Wei, C., Shi, Z., Zhu, J. (2018). Study on the diagnosis of small hepatocellular carcinoma caused by hepatitis B cirrhosis via multi-slice spiral CT and MRI. *Oncology Letters, 15(1),* 503–508. DOI 10.3892/ol.2017.7313.
3. Liu, J., Fan, H., Qiu, G. P. (2017). Vascular permeability determined using multi-slice spiral CT perfusion can predict response to chemoradiotherapy in patients with advanced cervical squamous cell carcinoma. *International Journal of Clinical Pharmacology and Therapeutics, 55(7),* 619–626. DOI 10.5414/CP202847.
4. Peng, N., Wang, X., Zhang, Z., Fu, S., Fan, J. et al. (2016). Diagnosis value of multi-slice spiral CT in renal trauma. *Journal of X-Ray Science and Technology, 24(5),* 649–655. DOI 10.3233/XST-160585.
5. Xu, J., Shen, J., Ding, Y., Shen, H. Y., Zeng, Z. P. et al. (2012). The clinical value of combined use of MR imaging and multi-slice spiral CT in limb salvage surgery for orthopaedic oncology patients: Initial experience in nine patients. *Radiology and Oncology, 46(3),* 189–197. DOI 10.2478/v10019-012-0020-4.
6. Rau, S. E., Burgess, K. E. (2017). A retrospective evaluation of lomustine (CeeNU) in 32 treatment naïve cats with intermediate to large cell gastrointestinal lymphoma (2006–2013). *Veterinary and Comparative Oncology, 15(3),* 1019–1028. DOI 10.1111/vco.12243.
7. Moore, P. F., Rodriguez-Bertos, A., Kass, P. H. (2012). Feline gastrointestinal lymphoma: Mucosal architecture, immunophenotype, and molecular clonality. *Veterinary Pathology, 49(4),* 658–668. DOI 10.1177/0300985811404712.
8. Wu, W., Doan, N., Said, J., Karunasiri, D., Pullarkat, S. T. (2014). Strong expression of chemokine receptor CCR9 in diffuse large B-cell lymphoma and follicular lymphoma strongly correlates with gastrointestinal involvement. *Human Pathology, 45(7),* 1451–1458. DOI 10.1016/j.humpath.2014.02.021.
9. Parshley, D. L., LaRue, S. M., Kitchell, B., Heller, D., Dhaliwal, R. S. (2011). Abdominal irradiation as a rescue therapy for feline gastrointestinal lymphoma: A retrospective study of 11 cats (2001–2008). *Journal of Feline Medicine and Surgery, 13(2),* 63–68. DOI 10.1016/j.jfms.2010.07.017.
10. Xu, X., Wang, Z., Yu, Y., Wang, Y., Zhang, L. et al. (2014). Evaluation of the clinical characteristics and prognostic factors of gastrointestinal mucosa-associated lymphoid tissue (MALT) lymphoma. *Journal of Gastroenterology and Hepatology, 29(9),* 1678–1684. DOI 10.1111/jgh.12615.
11. Fujii, Y., Taniguchi, N., Koibuchi, H., Yasuda, Y., Nagai, H. (2008). Compressibility of gastrointestinal tract tumors during transabdominal sonographic examination: A clue to the diagnosis of gastrointestinal lymphoma. *Journal of Clinical Ultrasound, 36(2),* 59–62. DOI 10.1002/jcu.20393.
12. Zhang, G. P., Cao, P. F., Feng, L. J. (2014). Detection and clinical significance of genes in primary gastrointestinal MALT lymphoma. *Tumor Biology, 35(4),* 3223–3228. DOI 10.1007/s13277-013-1421-8.
13. Huang, W. T., Hsu, Y. H., Yang, S. F., Chuang, S. S. (2008). Primary gastrointestinal follicular lymphoma: A clinicopathologic study of 13 cases from Taiwan. *Journal of Clinical Gastroenterology, 42(9),* 997–1002. DOI 10.1097/MCG.0b013e3180f62b12.
14. Gupta, G., Agarwala, S., Thulkar, S., Shukla, B. (2011). Jejunal stricture: A rare complication of chemotherapy in pediatric gastrointestinal B-cell non-hodgkin lymphoma. *Journal of Pediatric Hematology/Oncology, 33(2),* e69–e71. DOI 10.1097/MPH.0b013e3181ef0402.
15. Fujishima, F., Katsushima, H., Fukuhara, N., Konosu-Fukaya, S., Nakamura, Y. et al. (2018). Incidence rate, subtype frequency, and occurrence site of malignant lymphoma in the gastrointestinal tract: Population-based analysis in Miyagi. *Japan Tohoku Journal of Experimental Medicine, 245(3),* 159–165. DOI 10.1620/tjem.245.159.
16. Gouldin, E. D., Mullin, C., Morges, M., Mehler, S. J. (2017). Feline discrete high-grade gastrointestinal lymphoma treated with surgical resection and adjuvant CHOP-based chemotherapy: Retrospective study of 20 cases. *Veterinary and Comparative Oncology, 15(2),* 328–335. DOI 10.1111/vco.12166.

17. Barzilai, M., Polliack, A., Avivi, I., Herishanu, Y., Ram, R. et al. (2018). Hodgkin lymphoma of the gastrointestinal tract in patients with inflammatory bowel disease: Portrait of a rare clinical entity. *Leukemia Research, 71(20),* 1–5. DOI 10.1016/j.leukres.2018.06.008.
18. Takahashi, T., Maruyama, Y., Saitoh, M., Itoh, H., Yoshimoto, M. et al. (2016). Synchronous occurrence of diffuse large B-cell lymphoma of the duodenum and gastrointestinal stromal tumor of the ileum in a patient with immune thrombocytopenic purpura. *Internal Medicine, 55(20),* 2951–2956. DOI 10.2169/internalmedicine.55.6712.
19. Smith, A. L., Wilson, A. P., Hardie, R. J., Krick, E. L., Schmiedt, C. W. (2011). Perioperative complications after full-thickness gastrointestinal surgery in cats with alimentary lymphoma. *Veterinary Surgery, 40(7),* 849–852. DOI 10.1111/j.1532-950X.2011.00863.x.
20. Crouse, Z., Phillips, B., Flory, A., Mahoney, J., Richter, K. et al. (2018). Post-chemotherapy perforation in cats with discrete intermediate- or large-cell gastrointestinal lymphoma. *Journal of Feline Medicine and Surgery, 20(8),* 696–703. DOI 10.1177/1098612X17723773.
21. Ohnishi, N., Takata, K., Miyata-Takata, T., Sato, Y., Tari, A. et al. (2016). CD10 down expression in follicular lymphoma correlates with gastrointestinal lesion involving the stomach and large intestine. *Cancer Science, 107(11),* 1687–1695. DOI 10.1111/cas.13031.
22. Zheng, L., Shin, J. H., Han, K., Tsauo, J., Yoon, H. K. et al. (2016). Transcatheter arterial embolization for gastrointestinal bleeding secondary to gastrointestinal lymphoma. *Cardiovascular and Interventional Radiology. Journal of Imaging in Diagnosis and Treatment, 39(11),* 1564–1572. DOI 10.1007/s00270-016-1422-2.
23. Takata, K., Miyata-Takata, T., Sato, Y., Iwamuro, M., Okada, H. et al. (2018). Gastrointestinal follicular lymphoma: Current knowledge and future challenges. *Pathology International, 68(1),* 1–6. DOI 10.1111/pin.12621.